ELSEVIER

Contents lists available at ScienceDirect

Estuarine, Coastal and Shelf Science

journal homepage: www.elsevier.com/locate/ecss



Marsh edge erosion and associated carbon dynamics in coastal Louisiana: A proxy for future wetland-dominated coastlines world-wide



Yadav Sapkota, John R. White*

Wetland and Aquatic Biogeochemistry Laboratory, Department of Oceanography and Coastal Sciences, Louisiana State University, Baton Rouge, LA, USA

ARTICLE INFO

Keywords: Barataria basin Wetlands Marsh edge Erosion Carbon Emission

ABSTRACT

Coastal wetland loss through marsh edge erosion is a serious problem in Louisiana. The majority of studies on coastal land loss use aerial and satellite photographic analysis while field and site-specific measurements are limited. The aim of this study was to spatially and temporally measure coastal marsh edge erosion and investigate factors responsible for differences in erosion including shoreline orientation, soil physio-chemical properties, and wind speed and duration. A total of 33 transects across six island sites in northern Barataria Basin, Louisiana were established. Transects on shorelines facing different compass directions were measured for erosion for up to 2 years. Soils were analyzed for physiochemical properties including bulk density, organic matter, total carbon, nitrogen, and phosphorus. Bathymetric surveys were conducted to determine the extent of the erosive bay bottom profile. In addition, ¹⁴C dating of the basal organic matter (1.5–1.6 m) was conducted. Erosion rates ranged from 49.27 to 324.85 cm y^{-1} with a mean value of 141.69 \pm 22.45 cm y^{-1} . As expected, erosion rates were significantly different (p < 0.001) between protected and unprotected sites. The erosion rate was not correlated with wind speed (r = -0.07), weakly correlated with compass direction of shoreline (r = 0.25) and water level (r = 0.25) but strongly correlated with duration of wind (r = 0.60). Erosion rate was negatively correlated (r = -0.45) with bulk density and positively correlated with organic matter content (r = 0.42) of the top 40 cm of the soil. Over time, the marsh is eroded down to a depth of 1.5 m, which correlates to annual loss of 1.82 \pm 0.29 m³ volume of marsh per meter shoreline length including a loss of organic matter $(141.5 \pm 22.55 \,\mathrm{kg}\,\mathrm{m}^{-1})$ and carbon $(63.32 \pm 10.09 \,\mathrm{kg}\,\mathrm{m}^{-1})$ previously preserved for up to 850 years. As a consequence, annual CO_2 emissions for Barataria Basin were estimated to be 1.56 \pm 0.26 million tCO_2 e y^{-1} . Results can inform coastal managers as to the most vulnerable marshes to target restoration efforts. Due to high relative sea level rise in coastal Louisiana, these results can also be used to inform the world's stable coastlines on the relative vulnerability of their coastal marshes in the near future, due to projected eustatic sea level. Consequently, the eroding coastlines across the globe may be a significant source of CO2 emissions in near future, as millennial age stored soil carbon is released in a relatively short time, potentially overwhelming human efforts to slow rising atmospheric CO2 levels.

1. Introduction

Coastal wetlands provide numerous ecosystem services including habitat for diverse flora and fauna, nutrient removal and cycling, carbon sequestration and storage, resources for recreation, and protection from flood and storm surge (Theuerkauf et al., 2015; Reddy and DeLaune, 2008; Tonelli et al., 2010). Despite their profound importance, coastal wetlands are threatened due to sea level rise, local subsidence, edge erosion, lack of riverine sediment supply, hurricanes, human development (Theuerkauf et al., 2015; Priestas et al., 2015; DeLaune and White, 2012), and peat collapse (Chambers et al., 2019; Berkowitz et al., 2018). Marsh edge erosion is one of the primary

drivers of shoreline retreat in wetland-dominated coastlines (Morton et al., 2009; Wilson and Allison, 2008; Nyman et al., 1994) which has been accelerated by sea level rise, subsidence and limited sediment supply (Morton et al., 2009; DeLaune and White, 2012; Blum and Roberts, 2009; Day et al., 2000).

The Louisiana coast is a wetland-dominated system comprising of \sim 40% of the coastal wetland in the contiguous US but represents \sim 80% of the coastal wetland loss. From 1932 to 2016, almost 25% (4,833 km²) of the existing coastal wetlands were converted to open water (Couvillion et al., 2017). Coastal Louisiana is experiencing high relative sea level rise (\sim 12 mm y $^{-1}$) to the level that other wetland-dominated coastline may experience within next 50–60 years

^{*} Corresponding author.

E-mail address: jrwhite@lsu.edu (J.R. White).

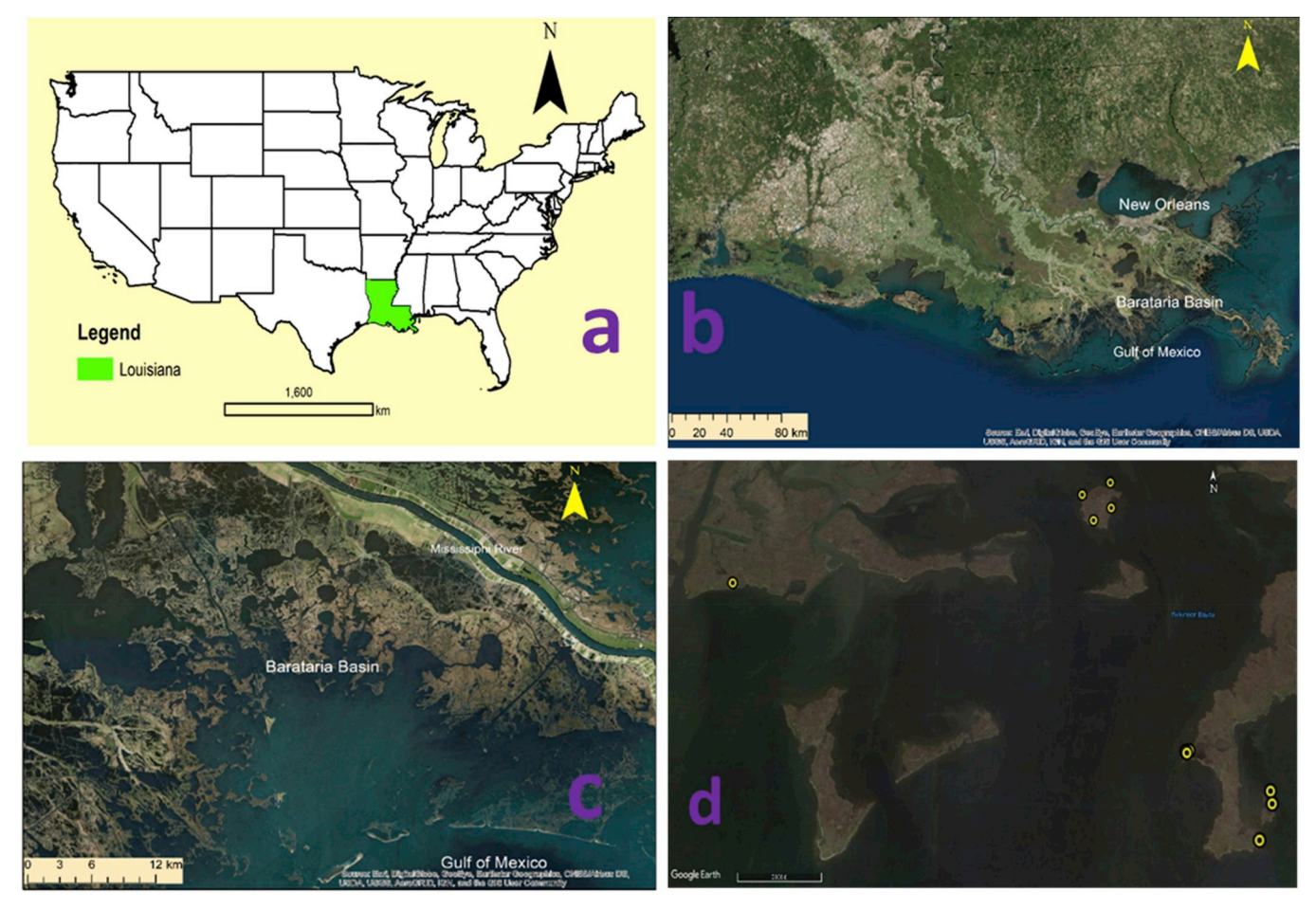


Fig. 1. Location of study site. (a) Map of contiguous United States, (b) Location of Barataria basin in Louisiana, (c) Barataria basin, and (d) Erosion measurement sites in Barataria basin.

(Jankowski, 2017; Penland and Ramsey, 1990). This high relative sea level rise and wetland loss at present make coastal Louisiana an ideal place to study potential carbon loss from other wetland-dominated coastlines in the near future. The high relative sea level rise results in the submergence of coastal wetlands and promote carbon mineralization (Steinmuller et al., 2019: Steinmuller and Chambers, 2019; DeLaune and White, 2012). The high relative sea level rise may also promote carbon accumulation in the presence of additional accommodation space (Rogers et al., 2019; Schuerch et al., 2018), however, may be limited by the reduced sediment load of the Mississippi River (Blum and Roberts, 2009).

Barataria Basin, an estuary in southeast Louisiana is one of the most vulnerable sites of marsh edge erosion (Morton et al., 2009; Wilson and Allison, 2008). The erosion has been likely enhanced by initial subsidence lowering the marsh surface to a position that is susceptible to erosion by waves (Morton et al., 2009). The greater exposure of marsh edges to open water in the Barataria basin may exacerbate edge erosion. The edge erosion has also been accelerated by hurricanes and anthropogenic activities including channelization and construction activities within the Mississippi River Delta complex (Browne, 2017). Erosion significantly increased in some areas after the 2010 BP Deepwater Horizon Oil spill due to the impact on belowground biomass growth (Turner et al., 2016; McClenachan et al., 2013).

In addition to marsh edge erosion, ponding, pond expansion, submergence, and vegetation dieback has a significant contribution to the wetland and subsequent carbon loss in wetland dominated coastlines (Ortiz et al., 2017; Spivak et al., 2017; Mariotti, 2016; DeLaune and White, 2012). Though there is consensus on the dominance of marsh edge erosion as the primary mechanism of wetland loss in Barataria Basin (Morton et al., 2009; Wilson and Allison, 2008), actual field measurements are limited and factors influencing erosion haven't been well identified. Most of the monitoring and predictions are based on aerial photography and satellite images analysis (Browne, 2017; Couvillion et al., 2017; Wilson and Allison, 2008). The geomorphological setting of the fragmented islands in the northern part of the Barataria Bay is complex. Although the wind wave comes primarily from the south-eastern part of the bay, erosion is visible on the marsh islands facing all compass directions. Field-based measurement of edge erosion on variable spatial and temporal scales may be useful to identify characteristics which identify the vulnerable sites of edge erosion to be targeted for coastal restoration.

Studies on other tidal salt marshes have identified wind waves as the primary factor responsible for marsh edge erosion (Wang et al., 2017; Sharma et al., 2016; McLoughlin et al., 2015; Tonelli et al., 2010; Wolters et al., 2005). Some studies have indicated that the rate of edge erosion is linearly related to the power of the incident wave (Leonardi et al., 2016; Marani et al., 2011). The wave thrust on the marsh edge is strongly related to the tidal level, which continues to increase eventually leading to submergence of marsh surface (Tonelli et al., 2010).

Studies on other coastlines have also identified soil physio-chemical properties (Wang et al., 2017; McLoughlin et al., 2015; Feagin et al., 2009; Cowart et al., 2010; Morton et al., 2009) and vegetation cover (Wang et al., 2017; Feagin et al., 2009) as the secondary factors of marsh edge erosion. In some cases, vegetation may not directly reduce erosion but can influence sediment characteristics thereby indirectly preventing erosion (Feagin et al., 2009).

Most of the studies on factors of marsh edge erosion have been concentrated on tidal marshes however, coastal Louisiana is a microtidal system with a diurnal tidal regime (Georgiou et al., 2005). Most of the waves interacting with the marsh edges are generated locally within the shallow bay with no significant tidal or river current. Thus, the factors responsible for edge erosion in this setting may be different than found for other tidal marshes.

Marsh edge erosion converts marsh into mudflats which release stored sediment, carbon, and nutrients resulting into potentially serious ecological disturbances and economic consequences (Pendleton et al., 2012; Macreadie et al., 2013; Sharma et al., 2016). The organic matter released into the estuary through marsh edge erosion produces a significant impact in biogeochemical cycles in the estuary and continental shelf affecting coastal carbon budgets (Wilson and Allison, 2008; Macreadie et al., 2013).

The goal of this study was to assess factors responsible for differences in erosion (shoreline orientation, or soil composition, or wind speed and duration) and quantify the erosion-driven carbon and nutrient export into the Barataria Bay.

2. Methods

2.1. Site selection

Barataria Basin in southeast Louisiana is disconnected from Mississippi River by extensive levees and consequently, limited in sediment supply. Continuous erosion with no new land building due to a lack of river sediment supply has resulted in rapid wetland land loss in this area. The entire basin has lost approximately $1172 \, \mathrm{km}^2$ of land in the period between 1932 and 2016 (Couvillion et al., 2017). Six islands located on the northern part of Barataria Basin (Fig. 1) were selected for erosion measurement. A total of 33 transects were established over 11 sites. These sites had marsh edges facing six different compass directions (Table 1). The sites that directly faces open bay were designated as unprotected sites while the sites that are adjacent to the shallow ponded areas, generally protected in the lee of other islands, were classified as protected sites (Table 1).

2.2. Erosion measurement

Three erosion poles were set at each transect (Fig. 2). The first pole (close to the edge) was set 1 m apart from the edge, the second pole was 1 m from the first and third pole was 1 m apart from the second. The distance from the first pole to the edge was measured at least once every two months from all transects. As the erosion proceeded and the first pole fell into the bay, the pole was relocated 1 m apart from the end of the transect. The record of erosion and loss of poles were documented in a field book.

2.3. Micro-topography assessment

Side scans and the bathymetric surveys were conducted along transects perpendicular to the marsh edge up to $200\,\mathrm{m}$ into the estuary,

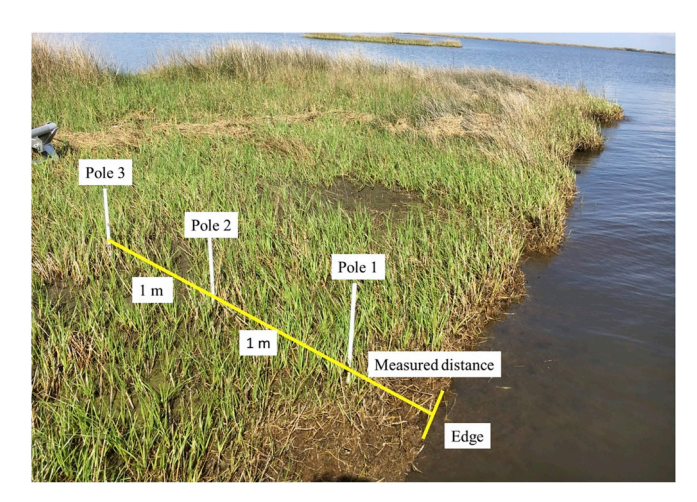


Fig. 2. Layout of erosion poles in an erosion measurement transect.

in September 2018 using Humminbird GPS (Helix 9 Chirp Mega DI GPS G2N, Johnson Outdoors Marine Electronics Inc., Eufaula, AL). Side scans measured the relative roughness of the recently eroded and historically eroded estuarine bottom. The bathymetric survey measured the depth of the estuary relative to the marsh surface. The measurements were taken in six sites (Ben, Hav, Yad 1, Yad 2, Yad 3 and weeks). In addition, the depths up to 2 m from the marsh edge, out of reach of the fathometer, were measured using a metered pole.

2.4. Wind speed, direction and gage height

The hourly wind speed, direction, and gage height data for the year 2017 and 2018 were downloaded from the nearest United States Geological Survey (USGS) station (07380251, North of Barataria Bay, LA) located approximately 3–5 km south and southwest of the erosion measurement sites. The wind measurement stations located offshore in the bay provide reliable estimate of the estuarine wind (Mariotti et al., 2018). Average wind speed and duration of wind in each compass direction was calculated from the data. In addition, average gage height when wind was blowing in different compass direction was also calculated.

2.5. Soil sampling

Forty-centimeter-deep soil cores were collected during summer and fall 2018 from 30 transects of 10 sites. Nine soil cores (\sim 1m long) were collected from three sites in Yad island. All the samples were collected 1 m inland from the marsh edge in each transect. A polycarbonate core tube (1.7 m \times 7.6 cm diameter) was used to extract soil samples via the push core method. Soils were extruded in the field into 10 cm intervals and placed and sealed in zip lock bags. Samples were stored on ice and

Table 1Erosion measurement sites in Barataria Basin, Louisiana.

Site No.	Sites	Measurement duration (year)	Shoreline orientation	GPS Coordinate of sites	Nature of site	
1	Ben	2	East	29.443585°, -89.899836°	Unprotected	
2	Hav	2	South-East	29.441510°, -89.901437°	Unprotected	
3	Week	2	South	29.459258°, -89.946278°	Unprotected	
4	YAD 1	1	North	29.446837°, -89.905628°	Unprotected	
5	YAD 2	1	West	29.446790°, -89.905927°	Unprotected	
6	YAD 3	1	South	29.446688°, -89.905857°	Unprotected	
7	MP 1	1	South	29.464972°, -89.911340°	Protected	
8	MP 2	1	West	29.467530°, -89.912215°	Protected	
9	MP 3	1	North-East	29.468791°, -89.909128°	Protected	
10	MP 4	1	East	29.466200°, -89.909385°	Protected	
11	Brian	2	East	29.444340°, -89.899737°	Unprotected	

immediately transported to Louisiana State University (LSU), and stored at 4 °C until analysis.

2.6. Sample processing for soil physio-chemical properties

Each sample was initially weighed, homogenized, and a subsample was taken for further analysis. The 40 cm long cores were analyzed for moisture content, bulk density, and % organic matter. The 1-m-long cores were analyzed for moisture content, bulk density, percent organic matter (% OM), total carbon (TC), total nitrogen (TN), and total phosphorus (TP). Gravimetric moisture content was determined by weighing 20–30 g subsample of soil before and after drying at 60 °C in a forced air oven until a constant weight was achieved. The bulk density of each sample was determined by calculating the total dry weight of the sample and then dividing by the volume of the 10 cm section of the core (384.85 cm³). The dried samples were ground using a mortar and pestle. Total carbon and nitrogen were determined from the ground subsample using an elemental combustion system (Costech Analytical Technologies, Valencia, CA). The percent organic matter was determined by the loss on ignition (LOI) technique, where 0.2-0.5 g samples were weighed in 50 ml glass beakers and ashed in a muffle furnace at 550 °C for 4 h. The % OM was calculated by dividing the weight of sample lost on ignition by the pre-ash weight. Total phosphorus was determined by digesting the ashed samples following Andersen (1976) and analyzed colorimetrically (USEPA, 1993) using a SEAL AQ2 Automated Discrete Analyzer (SEAL Analytical Inc, Mequon, Wisconsin) with a detection limit of $0.002 \,\mathrm{mg}\,\mathrm{P}\,\mathrm{L}^{-1}$.

2.7. 14C dating of the organic matter

Two samples were taken, one from Yad 2 (N29.446790°, W89.905927°) and one from Ben Island (N29.443390°, W89.899816°) at the depth of 1.5–1.6 m deep in the marsh and sent to Beta Analytics LLC, Miami, FL for ¹⁴C dating on the decayed plant materials. Samples were pretreated with acid/alkali/acid to remove carbonates and humic acids and fraction isolated as-fine grained high carbon sediment and decayed plant materials. The decayed plant remains were chosen to undergo ¹⁴C analyses. The conventional radiocarbon age (uncalibrated age) were corrected for total fractionation effects. The calibration of radiocarbon age (yBP) to calendar years (cal AD) was performed using BetaCal 3.21 which utilize INTCAL13 database (Reimer et al., 2013) and high probability density range method (HPD) (Bronk Ramsey, 2009).

2.8. Statistical analysis

Statistical analysis was performed using Microsoft Excel, JMP (Version Pro 14.1, SAS Institute Inc., Cary, NC) and R in R Studio (R Foundation for Statistical Computing, Vienna, Austria). Erosion rates were obtained by regressing measured erosion with time. Erosion rates, bulk density and organic matter between protected and unprotected sites were compared using Welch two-sample *t*-test in R. In addition, the correlation coefficients were obtained between erosion rates and compass direction of the site, bulk density and organic matter content of top 40 cm depth of soil, wind speed, wind duration, and gage height from IMP

We used an equilibrium profile model after Wilson and Allison (2008) to estimate the amount of erosion-driven sediment, organic matter, and nutrient export into the estuary. We constructed an equilibrium profile of the sites by first plotting bathymetric data. The depth of the estuary was plotted against distance from the marsh edge up to 200 m into the estuary. The depth of the estuary adjacent to the Yad 1 and Yad 3 were relatively shallow than the estuary adjacent to Yad 2, Ben and Hav. The bathymetry of the Yad 1 and Yad 3 ran through the lee of adjacent marshes and may represent the condition of the protected sites. Two equilibrium profiles of the bay were prepared 1)

Table 2
Marsh edge erosion rate in different sites.

Site No.	Sites	Erosion rate (cm y ⁻¹)
1	Ben	141.62 ± 24.44
2	Hav	241.75 ± 30.87
3	Week	237.86 ± 47.99
4	YAD 1	152.33 ± 11.50
5	YAD 2	221.96 ± 55.93
6	YAD 3	76.77 ± 4.84
7	MP 1	90.52 ± 21.36
8	MP 2	95.75 ± 6.27
9	MP 3	106.58 ± 13.73
10	MP 4	72.27 ± 6.22
11	Brian	121.14 ± 23.84

protected bathymetric profile combining the profile of Yad 1 and Yad 3, and 2) unprotected bathymetric profile combining the profile of Yad 2, Ben and Hav. Both, protected and unprotected bathymetric profiles were well fitted with a logarithmic function.

The annual export of sediment and associated organic matter by erosion was calculated using equation from Sorensen (2006)-

$$V = h(dx)(dy)$$

where V is the volume of eroded marsh, h is the depth of the estuary where bottom slope runs to almost zero and is not considered erosional, dy is the lateral displacement of the profile due to erosion and dx is the shoreline length. This equation was also used by Wilson and Allison (2008) to estimate sediment export by erosion in Barataria and Breton Sound Basin of Louisiana using historical erosion rates predicted from satellite and aerial images.

3. Results

3.1. Erosion rate

The edge erosion rates ranged from 49.27 to 324.85 cm y^{-1} with a mean value of 141.69 \pm 22.45 cm y^{-1} (Table 2). The protected sites had erosion rates ranging from 49.27 to 127.38 cm y^{-1} with a mean value of 91.28 \pm 6.85 cm y^{-1} while the unprotected site had erosion rates ranging from 67.16 to 324.85 cm y^{-1} with a mean value of 170.49 \pm 16.92 cm y^{-1} . Erosion rates were significantly higher (p < 0.001) at unprotected sites compared to protected sites.

Erosion rates were weakly correlated (r=0.25) with compass direction of shoreline. In protected sites, the south and east facing edges were least eroding while north-east facing marsh edges experienced highest erosion rates. However, in the unprotected sites, the east and north facing edges were least eroding while south-east, south, and west facing edges had the highest erosion rates suggesting a complex pattern of wave refraction.

3.2. Wind speed, direction and gage height

The duration of the wind was greatest (55%) from 67.5 to 202.5° (east and south) with dominant blow (24%) in the south-east direction (112.5–157.5°). The duration of wind was least from the west (247.5–292.5°) and north-west (292.5–337.5°) direction with the share of 6.8 and 7.9% respectively. Wind speed ranged from 0.05 to 19.54 m s $^{-1}$ with an average speed of 5.43 \pm 0.06 m s $^{-1}$. The average speed of wind blowing from southerly direction was 4.75 \pm 0.10 m s $^{-1}$ and that from the north was 6.60 \pm 0.10 m s $^{-1}$ (Fig. 3). The duration of the northerly wind was less but the velocity was highest especially during the winter season. The duration of the southerly wind was high but the magnitude was low with some extreme values related to storms (Fig. 3).

Gage height ranged between $-0.41\,\text{m}$ and $1.19\,\text{m}$ with the mean value of $0.45\,\pm\,0.004\,\text{m}$. Gage height was least $(0.33\,\pm\,0.06\,\text{m})$

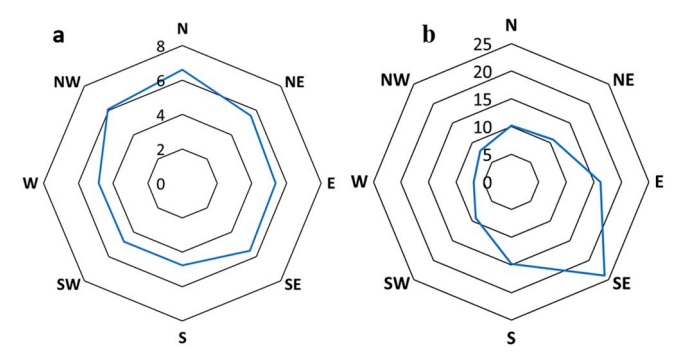


Fig. 3. (a) Average wind speed (m/s), and (b) duration (%) of wind in different directions in northern part of Barataria Basin. Hourly wind speed and direction data of year 2017 and 2018 were downloaded from USGS station # 07380251, North of Barataria Bay, LA.

during northerly winds and was highest (0.50 \pm 0.05 m) when the wind was blowing from south-east direction. The erosion rate was not correlated with wind speed (r = -0.07), weakly correlated with gage height (r = 0.25) but strongly correlated with wind duration (r = 0.60).

3.3. Soil physiochemical properties

3.3.1. The 40 cm soil cores

The bulk density and organic matter content in top 40 cm soil cores are presented in Table 3. Bulk density was significantly greater (p = 0.002) in protected sites whereas organic matter content was significantly greater (p = 0.005) in unprotected sites. One unprotected site with south facing marsh edge (Week's island) was excluded in bulk density and %OM comparison between protected and unprotected sites due to the presence of anomalously high bulk density (0.44 gm cm $^{-3}$) and low organic matter (12.64%), likely influenced by close proximity to a former distributary channel of the Mississippi River.

Erosion rate was negatively correlated (r=-0.45) with bulk density and positively correlated with organic matter content (r=0.42) of the top 40 cm of the soil.

3.3.2. One-meter soil cores

Depth was the significant predictor (p < 0.001) of bulk density, % organic matter, total carbon (TC), total nitrogen (TN), and total phosphorus (TP). Generally, bulk density increased from the surface to 40-50 cm, then decreased (Table 4). A similar trend of bulk density was reported by Haywood (2018). Bulk density was strongly negatively correlated with organic matter content and strongly positively correlated with total carbon and total nitrogen (Table 5). With depth, organic matter remained relatively constant up to 40-50 cm, increased by approximately 45% at 50-60 cm, and again remained almost constant thereafter. Organic matter content was strongly correlated with total carbon and total nitrogen. Total carbon exhibited a similar trend of organic matter. Similarly, total nitrogen also remained relatively constant up to 40-50 cm and then gradually increased. Total P (TP) was highest at the surface, decreased up to 40-50 cm, slightly increased at 50-60 cm and remained relatively constant thereafter. The relatively sharp change at 40-50 cm depth might indicate change in marsh type or

Table 3 Physiochemical properties of top 40 cm soils of different sites.

Sites	Bulk density (g cm ⁻³)	Organic matter (%)
Unprotected	0.28 ± 0.02	26.76 ± 1.02
Protected	0.34 ± 0.05	19.98 ± 2.98
Average	0.30 ± 0.02	22.64 ± 1.96

river influence.

3.4. 14C dating of the organic matter

The calibrated age of the organic matter at the soil depth interval of 1.5–1.6 m from Yad 2 was 825 \pm 85 years before present (cal yBP; BP is 1950) and that of Ben island was 738 \pm 52 cal yBP (Table 6). The mean age of organic matter was 781 \pm 111 cal yBP. In 2019, the age of the organic matter was 850 \pm 111 which represents long term accretion rate of 1.82 \pm 0.24 mm y⁻¹. The age of the organic carbon estimated by this study is consistent with the dates estimated by Bomer et al. (2019) from the sites approximately 20 km northwest of our study sites in Barataria Basin. They estimated the age of organic matter at the soil depth of 0.60–0.61 m to be 235 \pm 132 cal yBP which represent the long term accretion rate of 1.85 \pm 0.6 mm y⁻¹. Likewise, the age of organic matter at the soil depth of 1.15–1.16 m was 998 \pm 92 cal yBP which represent the long term accretion rate of 1.07 \pm 0.08 mm y⁻¹. The δ^{13} C signatures in our samples (Table 6) indicate that the organic matter stored at the depth of 1.5-1.6 m was from intermediate marshes (Chmura et al., 1987; DeLaune, 1986), which are now salt marshes dominated by Spartina alterniflora at the surface.

3.5. Microtopography

The surface of the bottom sediment was rough from the marsh edges to the point into the estuary where the surface slope approaches to zero. The depth of the estuary at the edge of the marsh, 5 cm into the open water, ranged from 0.22 to 0.60 m with the mean of 0.36 \pm 0.02 m. The depth gradually increased until 150–200 m into the estuary and then generally flattens out except week's island where the surface of the estuary flattens out (1.1 m deep) approximately at 5 m and demonstrate alternate pattern of decrease and increase in depth beyond 60 m from the marsh edge. Week's island may be a headland site of a former distribution channel of the Mississippi River and was thus excluded in constructing equilibrium bathymetric profile. The maximum depth of the estuary adjacent to protected sites was 1.07 m and that of unprotected sites was 1.5 m at the distance of 200 m (Fig. 4).

4. Discussion

4.1. Erosion rate and the factors of erosion

During this study, marsh edge eroded at variable rates within Barataria basin. The variability of the erosion rate was attributed to a number of factors including wind duration and soil physio-chemical properties. In addition, the complex geomorphological setting of the basin appears to be influencing the erosion rates. The sites adjacent to the open bay (unprotected sites) experience greater erosion rates than the protected sites located adjacent to the shallow water bodies in the northern part of the basin. This difference is likely affected by the increased fetch of unprotected sites. The shallow bathymetry and small fetch produce waves with small power that induce slow erosion (Valentine and Mariotti, 2019; Tonelli et al., 2010). Likewise, the waves couldn't travel long distance due to barriers and the low power waves are locally generated. However, a substantial rate of erosion (91.28 \pm 6.85 cm y $^{-1}$) was observed in unprotected sites mainly due to locally generated waves and wave refraction.

Erosion rate was strongly correlated to the duration of the wind, which predominantly comes from the south-east direction, indicating prolonged wind from this direction will continuously erode marsh edge. The duration of wind blowing from south-east direction was maximum followed by south and east direction in Barataria Basin (Fig. 3b). Thus, the shorelines facing south-east, south and east are more vulnerable to edge erosion by wind waves. However, all marsh edges erode regardless of direction and wind speeds. Leonardi et al. (2016) also noted that edge erosion occurs continuously, even under small breeze and is

Table 4 Physiochemical properties of 1-m-deep soil cores (n = 9).

Depth	Bulk Density (g cm ⁻³)	Organic Matter (%)	Total Carbon (g kg ⁻¹)	Total Nitrogen (g kg ⁻¹)	Total Phosphorus (mg kg ⁻¹)
0–10	0.27 ± 0.004	27.52 ± 0.51	121.37 ± 2.1	6.32 ± 0.13	475.11 ± 6.32
10-20	0.27 ± 0.004	29.96 ± 0.68	131.06 ± 4.1	6.61 ± 0.14	449.62 ± 5.36
20-30	0.3 ± 0.003	24.15 ± 0.3	101.21 ± 1.52	5.95 ± 0.08	406.13 ± 6.92
30-40	0.26 ± 0.004	26.59 ± 0.41	117.54 ± 2.71	6.47 ± 0.09	420.34 ± 4.47
40-50	0.29 ± 0.011	25.37 ± 0.96	111.04 ± 4.47	6.05 ± 0.22	393.31 ± 7.76
50-60	0.21 ± 0.002	36.95 ± 0.69	168.46 ± 3.3	8.72 ± 0.14	421.93 ± 4.43
60–70	0.17 ± 0.002	43.52 ± 0.73	198.83 ± 1.88	10.53 ± 0.07	401.55 ± 5.39
70-80	0.17 ± 0.002	41.56 ± 0.39	186.37 ± 2.62	10.41 ± 0.11	405.46 ± 6.65
80-90	0.2 ± 0.005	37.99 ± 1	174.91 ± 4.46	10.22 ± 0.22	412.33 ± 6.48
90–100	0.23 ± 0.004	34.61 ± 0.8	157.95 ± 3.89	9.44 ± 0.2	425.03 ± 5.68

Table 5Correlation (r) matrix of the soil physiochemical properties of 1 m cores.

	BD	MC	%OM	Total C	Total N
MC	-0.98				
%OM	-0.90	0.91			
Total C	-0.89	0.90	0.96		
Total N	-0.89	0.90	0.91	0.94	
Total P	0.07	-0.11	0.00	0.04	-0.04

BD = Bulk Density, MC = Moisture Content, OM = Organic Matter.

mainly affected by the moderate storms. The small and shallow water waves continuously erode marsh edge and erosion rate will increase if wind blows for prolonging duration of time. Valentine and Mariotti (2019) measured marsh edge erosion in two protected sites facing each other in Barataria Basin and reported that erosion rate in north facing edge was twice the rate of south facing edge. This variation in erosion rate is attributed to the water level in the bay especially low water level during northerly wind. Low water level reduces the chances of wave overshooting over the marsh consequently impacting the marsh edge with higher wave thrust (Valentine and Mariotti, 2019; Tonelli et al., 2010).

The erosion rate was significantly negatively correlated with the bulk density, and positively correlated with organic matter content, of the surface soil of the marsh soil. With the increase in organic matter content bulk density of the soil decreases thus increasing the susceptibility of the marsh edge to erosion. The lower strength of the marsh platform might be an additional driver of the continuous erosion caused by the wind waves. Our result is consistent with the studies relating shoreline erosion with the soil composition that determines shear strength and soil erodibility (Wang et al., 2017; Feagin et al., 2009; Morton et al., 2009, Valentine and Mariotti, 2019). These studies indicate that the high bulk density and presence of the plant roots increases shear strength and decreases soil erodibility.

The increase in water depth and wave heights resulting from sea level rise is predicted to cause more rapid erosion of marsh edge in future scenarios (Mariotti et al., 2010). Coastlines formed by vertical accretion from organic matter and river sediment, like coastal Louisiana, are more vulnerable to erosion than rocky shorelines (Su et al., 2017). Continuous erosion of the marsh edge exposes new surface for the action of wave energy, until the marsh is converted into open water.

4.2. Process of marsh edge erosion

Wind creates waves and tides that encounter marsh edges, loosen underlying fine sediments and lead to collapse of rooted pieces of edge into the open water (McLoughlin et al., 2015). The elevation of surface of the edge (0.36 \pm 0.02 m) adjacent to the estuary is the hot spot for wave attack and subsequent erosion. Due to the presence of thick vegetation and roots on top 10–20 cm of the soil, the marsh is undercut from below 20–30 cm into the marsh platform (Fig. 5). The hanging root mat remains intact for a period of time before wave action separates it from the marsh. As the wave attack continues, the hanging surface of the marsh platform slump down into open water (Fig. 6). Coincidentally, the submerged sloping surface (recently eroded marsh) in the estuary will continue to erode due to wave swash until the depth is beyond wave influence (1.28 \pm 0.22 m).

4.3. Consequences of erosion

4.3.1. Wetland loss

The $\delta^{13}C$ signatures in the soil organic matter indicated that sea level rise and river separation by levees has transformed the study sites to salt marshes, which were intermediate marshes before 850 years. The unprotected sites lying adjacent to open bay are eroding more rapidly (170.49 \pm 16.92 cm y $^{-1}$) than protected sites (91.28 \pm 6.85 cm y $^{-1}$) lying adjacent to shallow ponded area in the lee of other marsh islands. The rapidly eroding unprotected sites will be converted to open water more quickly than protected sites. Consequently, it is likely that the current protected sites will become exposed to the open bay and experience increased erosion rate in the future. Our study indicates that erosion is persistent on all sides of these islands. The shrinking from all sides has resulted in rapid loss of these small islands in the Basin and overall highest land loss rate in coastal Louisiana.

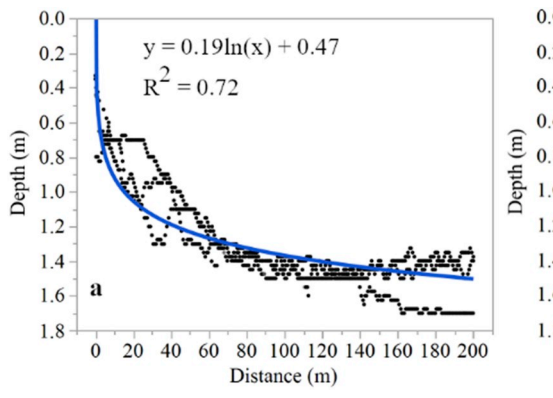
4.3.2. Organic matter and nutrients export

Our measurements estimated that annually $1.82 \pm 22.5 \, \text{m}^3$ volume of marsh per meter length of shoreline is being exported by marsh edge erosion, which is close to the estimate of $1.7 \, \text{m}^3$ per meter shoreline length estimate made by Wilson and Allison (2008) for Barataria Basin. We have also estimated that annually, $141 \pm 22.5 \, \text{kg}$ of organic matter per meter of shoreline length is exported into the open water which contains $63.32 \pm 10.09 \, \text{kg} \, \text{m}^{-1}$ organic carbon (Table 7).

These marshes contain high-quality organic matter down to the

Table 6
Radiocarbon dating results for decayed plant materials. Laboratory code: Beta - Beta Analytic, Miami, FL, USA. Calibration used- BetaCal3.21: High Probability Density Range Method (HPD): INTCAL13.

Site	Core Depth (cm)	Lab Code	δ ¹³ C (‰)	Uncalibrated Age (yBP)	Calibrated Age (cal AD)	Calibrated Age (cal yBP)
Yad 2	150–160	Beta-504739	-18.5	900 ± 30	1039–1210	825 ± 85
Ben	150–160	Beta-504740	-22.9	830 ± 30	1160–1264	738 ± 52



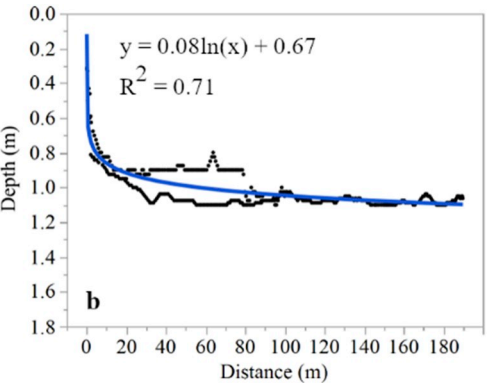


Fig. 4. Equilibrium bathymetric profile of a) unprotected sites b) protected sites. The depth is relative to the marsh surface. The black dots are the data points and the blue line is the model fit. The maximum depth of erosion was estimated 1.5 m for unprotected sites and 1.07 m for protected sites. (For interpretation of the references to color in this figure legend, the reader is referred to the Web version of this article.)

depth of 1.5 m that are susceptible to decomposition under aerobic condition (Steinmuller and Chambers, 2019). Vaccare et al., (2019) found reduced nitrate reduction rate in fringe and estuary bottom compared to the intact marsh. In addition, they found small amounts (8–10%) of organic matter on the bottom sediment of the estuary. No artifact of the marsh organic matter is observed at the bottom of the estuary. The bottom of the estuary contains mud with some refractory carbon in it. Thus the wetland soil organic matter, on being exposed to the aerobic water column conditions, is mineralized and emitted back into the atmosphere as $\rm CO_2$ (Steinmuller et al., 2019; Steinmuller and Chambers, 2019; DeLaune and White, 2012). Further work is essential to figure out the proportion of the carbon mineralized to the amount buried to the estuary bottom. Here we assumed 75% of the eroded carbon undergoes mineralization to estimate carbon emission from eroding marshes.

We used the reported land loss rate of $13.33\,\mathrm{km^2\,y^{-1}}$ for Barataria basin (Couvillion et al., 2017) and the mean erosion rate to estimate the shoreline length of the Barataria Basin (9387 km). Using shoreline length and carbon lost through a meter length of shoreline, total carbon emission from Barataria Basin was estimated to be 0.45 ± 0.07 million MT each year which is equivalent to 1.65 ± 0.26 million tCO $_2$ e. This estimate is for just one of 8 coastal basins of Louisiana. Other eroding coastal basins like Breton Sound and Terrebonne may have similar trends of CO $_2$ emission as they also experience coastal land loss. Thus, marsh edge erosion is a problem in coastal Louisiana and has been contributing to atmospheric CO $_2$ levels for almost a century and will continue in the future until some efficient means of restoration



Fig. 6. Marsh edge ready to slump down in Barataria Basin.

intervention is applied.

In addition to the carbon, from our sites annually 3.48 $\pm~0.55\,kg\,N$ and 181.53 $\pm~28.93\,g\,P$ per meter length of shoreline (Table 7) is being released into the bay. Accounting for the entire Barataria Basin, annually 32,666 $\pm~5162$ MT N and 1.7 $\pm~0.87$ MT P is being exported to the open water. This export of nutrients may contribute to eutrophication in the coastal estuaries and hypoxia in the northern Gulf of Mexico.

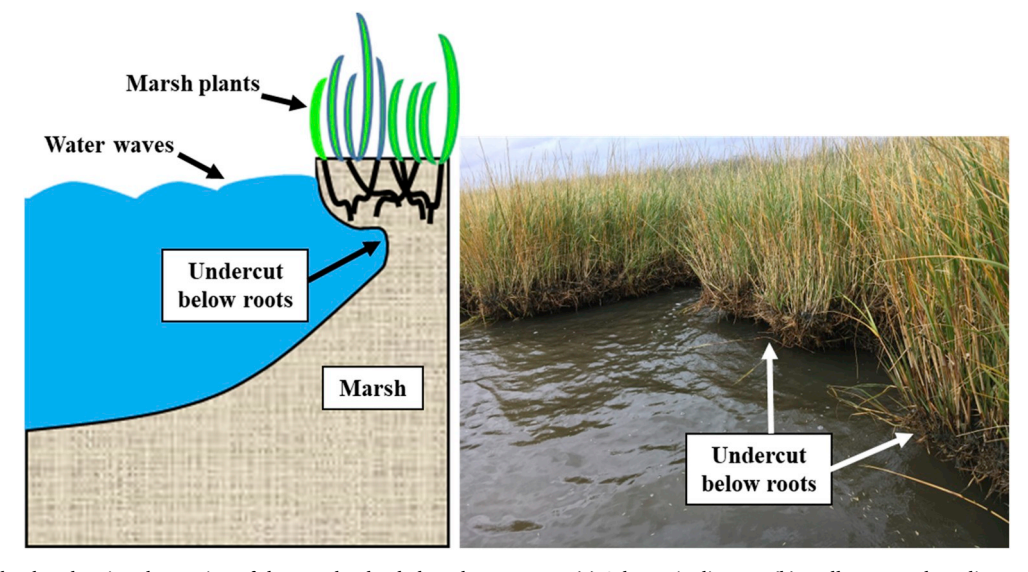


Fig. 5. Eroding marsh edge showing the cutting of the marsh edge below the root zone (a) Schematic diagram (b) Well vegetated eroding marsh edge in Barataria Basin, Louisiana.

Table 7Annual export of sediment, organic matter, carbon, nitrogen and phosphorus per meter of shoreline length into the open water due to marsh edge erosion.

Sites	Volume lost ($m^3 m^{-1}$)	Sediment (kg m^{-1})	Organic Matter (kg m ⁻¹)	Total C (kg m $^{-1}$)	Total N (kg m^{-1})	Total P (g m ⁻¹)
Protected Unprotected Average for the Basin	0.98 ± 0.07	232 ± 16.6	76.2 ± 5.4	34.1 ± 2.4	1.9 ± 0.1	97.8 ± 7
	2.56 ± 0.25	606 ± 59.2	199.1 ± 19.4	89.1 ± 8.7	4.9 ± 0.5	255.3 ± 24.9
	1.82 ± 0.29	431 ± 68.7	141.5 ± 22.6	63.3 ± 10.1	3.5 ± 0.6	181.5 ± 28.9

4.4. Coastal restoration and global implications

Presence of significant erosion rate throughout marshes indicate the relative vulnerability of the coastal wetlands in Louisiana and begs the attention of the coastal management authorities for the immediate implementation of restoration activities. The lower erosion rates in protected sites indicate that the erosion rate will be reduced if some sort of barrier or marsh creation project could be implemented to prevent direct impact of wind waves into the marsh edge. A continuous barrier construction has not been implemented in Louisiana to reduce erosion. The barriers may isolate the marshes compromising ecological services of these marshes. However, marsh creation using dredged materials is widely applied in Louisiana (CPRA, 2017; Wood et al., 2017). Likewise, higher bulk densities on least eroding sites indicate the potential of river sediment supply to increase marsh resilience. The large sediment diversion projects planned for coastal restoration in Louisiana will supply sediment to these eroding marshes, reduce fragmentation and help slow land loss in addition to building new land (Peyronnin et al., 2017; Roberts et al., 2015; DeLaune et al., 2013).

The carbon sequestration and preservation benefit of the coastal marshes might be utilized to increase the monetary value of the restoration benefits through the establishment of linkage with the global carbon credit markets. The restoration efforts preventing marsh loss not only capture annual carbon sequestration from the atmosphere but also prevents the loss of the carbon stored for up to 850 years. The value of the carbon prevented from going back into the atmosphere is several folds greater than the new carbon annually sequestered (DeLaune and White, 2012). However, the current wetland carbon credit methodologies do not include the credit for the preventing wetland loss except the methodology for the Mississippi Delta by Mack et al. (2012). The revised version (v2.0) of this methodology has included credit for preserving the top 50 cm of wetland soil. Our study has indicated that the vertical loss of the wetland soil carbon occurs up to 1.5 m depth. The existing wetland carbon credit methodologies may need to revise the credit for preventing wetland loss in LA. The inclusion/revision of the prevented wetland loss component in current carbon credit methodologies my increase the economic benefits from coastal restoration.

Our study indicates the severity of land loss that the Louisiana coast might face in the near future in the absence of the restoration efforts. The high relative sea level rise in Louisiana might accelerate this loss. Other large wetland coastal plains, like those in the Chesapeake Bay and Florida Everglades may lose land and stored carbon as sea level continues to rise. The Florida Everglades is a sediment starved system with low bulk density (White and Reddy, 1999, 2001) and is susceptible to erosion. Due to the extremely high relative sea level rise in coastal Louisiana, these results can also be used to inform the world's stable coastlines on the relative vulnerability of their coastal marshes soon to be affected in the near future as eustatic sea level reaches the levels of relative sea level in Louisiana (Jankowski, 2017; Horton et al., 2014). Efforts to mitigate atmopheric CO2 in the future might be muted as centuries of stored soil carbon in coastal weltands is released globally, further underscoring the importance of maintaining these C stores in place.

5. Conclusion

The phenomenon of coastal marsh erosion in Louisiana was

examined spatially and temporally. The erosion rate is primarily influenced by the duration of the wind not velocity as well as soil physiochemical properties and the physical location of the sites. This erosion is causing significant loss of carbon and nutrients altering the adjacent estuarine and atmospheric chemistry. Our study indicates that the wetland dominated coastlines worldwide my be significant source of carbon emission if current sea level rise predictions are realized. These findings can help inform coastal managers as to the most vulnerable marshes to erosion and can help target restoration efforts for dredge material placement and marsh creation. In addition, these findings might help to inform the future vulnerability of the wetland dominated coastlines that experience high relative sea level rise across the globe and suggest efforts should be made to preserve these vast carbon stocks from erosion and release to the atmosphere.

Acknowledgments

This work was funded under a collaborative National Science Foundation Chemical Oceanography Grant (#1636052). Y. Sapkota was funded by an Economic Development Assistantship from the Graduate School, Louisiana State University. We also acknowledge Eddie Weeks, Michael P. Hayes, Peter T. Mates, Jessica Vaccare, Benjamin J. Haywood, Havalend Steinmuller and Nia R. Hurst for help with fieldwork and Thomas Blanchard for laboratory assistance.

Appendix A. Supplementary data

Supplementary data to this article can be found online at https://doi.org/10.1016/j.ecss.2019.106289.

References

Andersen, J.M., 1976. An ignition method for determination of total phosphorus in lake sediments. Water Resour. 10, 329–331.

Berkowitz, J.F., VanZomeren, C.M., Piercy, C.D., White, J.R., 2018. Evaluation of coastal wetland soil properties in a degrading marsh. Estuar. Coast Shelf Sci. 212, 311–317.

Blum, M.D., Roberts, H.H., 2009. Drowning of the Mississippi Delta due to insufficient sediment supply and global sea-levelrise. Nat. Geosci. 2, 488–491. https://doi.org/ 10.1038/ngeo553.

Bomer, E.J., Bentley, S.J., Crawford, F., Hughes, J.E.T., et al., 2019. Sediment dynamics and stratigraphic evolution of middle Barataria bay and middle Breton Sound, Louisiana, USA: implications for the implementation of river-sediment diversions (In Review). Estuar. Coast Shelf Sci.

Bronk Ramsey, C., 2009. Bayesian analysis of radiocarbon dates. Radiocarbon 51 (1), 337–360. https://doi.org/10.1017/S0033822200033865.

Browne, J.P., 2017. Long-term erosional trends along channelized salt marsh edges. Estuar. Coasts 40, 1566–1575. https://doi.org/10.1007/s12237-017-0245-y.

Chambers, L.G., Steinmuller, Havalend E., Breithaupt, J.L., 2019. Toward a mechanistic understanding of "peat collapse" and its potential contribution to coastal wetland loss. Ecology 0. https://doi.org/10.1002/ecy.2720.

Chmura, G., Aharon, P., Socki, R., Abernethy, R., 1987. An inventory of 13C abundances in coastal wetlands of Louisiana, USA: vegetation and sediments. Oecologia 74, 264–271

Couvillion, B.R., Beck, H., Schoolmaster, D., Fischer, M., 2017. Land area change in coastal Louisiana (1932 to 2016) scientific investigations Map 3381. U.S. Geol. Surv. Sci. Investig. Map 3381 16. https://doi.org/10.3133/SIM3381.

Cowart, L., Walsh, J.P., Corbett, D.R., 2010. Analyzing estuarine shoreline change: a case study of cedar island, North Carolina. J. Coast. Res. 265, 817–830. https://doi.org/ 10.2112/JCOASTRES-D-09-00117.1.

CPRA, 2017. Louisiana's Comprehensive Master Plan for a Sustainable Coast. Coastal Protection and Restoration Authority. Baton Rouge, LA.

Day, J.W., Britsch, L.D., Hawes, S.R., Shaffer, G.P., Reed, D.J., Cahoon, D., 2000. Pattern and process of land loss in the Mississippi Delta: a spatial and temporal analysis of wetland habitat change. Estuaries 23, 425. https://doi.org/10.2307/1353136.

- DeLaune, R.D., 1986. The use of 813C signature of C-3 and C-4 plants in determining past depositional environments in rapidly accreting marshes of the Mississippi River deltaic plain, Louisiana, U.S.A. Chem. Geol. Isot. Geosci. Sect. 59, 315–320. https://doi.org/10.1016/0168-9622(86)90080-1.
- DeLaune, R.D., White, J.R., 2012. Will coastal wetlands continue to sequester carbon in response to an increase in global sea level?: A case study of the rapidly subsiding Mississippi river deltaic plain. Clim. Change 110 (1–2), 297–314. https://doi.org/10.1007/s10584-011-0089-6.
- DeLaune, R.D., Kongchum, M., White, J.R., Jugsujinda, A., 2013. Freshwater diversions as an ecosystem management tool for maintaining soil organic matter accretion in coastal marshes. Catena 107, 139–144.
- Feagin, R.A., Lozada-Bernard, S.M., Ravens, T.M., Moller, I., Yeager, K.M., Baird, A.H., 2009. Does vegetation prevent wave erosion of salt marsh edges? Proc. Natl. Acad. Sci. 106, 10109–10113. https://doi.org/10.1073/pnas.0901297106.
- Georgiou, I.Y., FitzGerald, D.M., Stonei, G.W., 2005. The Impact of Physical Processes along the Louisiana Coast. J. Coast. Res. 44, 72–89.
- Haywood, B.J., 2018. Molecular Level Interactions and Transformations of Natural Organic Matter within the Environment" (2018). LSU Doctoral Dissertations. pp. 4724. https://digitalcommons.lsu.edu/gradschool_dissertations/4724.
- Horton, B.P., Rahmstorf, S., Engelhart, S.E., Kemp, A.C., 2014. Expert assessment of sealevel rise by AD 2100 and AD 2300. Quat. Sci. Rev. 84, 1–6. https://doi.org/10.1016/i.quascirey.2013.11.002.
- Jankowski, K.L., 2017. Vulnerability of Louisiana's coastal wetlands to present-day rates of relative sea-level rise. Nat. Commun. 8, 1–7. 14792. https://doi.org/10.1038/ ncomms14792.
- Leonardi, N., Ganju, N.K., Fagherazzi, S., 2016. A linear relationship between wave power and erosion determines salt-marsh resilience to violent storms and hurricanes. Proc. Natl. Acad. Sci. 113, 64–68. https://doi.org/10.1073/pnas.1510095112.
- Mack, S.K., Lane, R.R., Day, J.W., 2012. Restoration of Degraded Deltaic Wetland of the Mississippi Delta. American Carbon Registry, Arlington VA.
- Macreadie, P.I., Hughes, A.R., Kimbro, D.L., 2013. Loss of "Blue Carbon" from Coastal Salt Marshes Following Habitat Disturbance. PLoS One 8, 1–8. https://doi.org/10.1371/journal.pone.0069244.
- Marani, M., D'Alpaos, A., Lanzoni, S., Santalucia, M., 2011. Understanding and predicting wave erosion of marsh edges. Geophys. Res. Lett. 38, 1–5. https://doi.org/10.1029/ 2011GL048995.
- Mariotti, G., Fagherazzi, S., Wiberg, P.L., McGlathery, K.J., Carniello, L., Defina, A., 2010.
 Influence of storm surges and sea level on shallow tidal basin erosive processes. J.
 Geophys. Res. Ocean. 115, 1–17. https://doi.org/10.1029/2009JC005892.
- Mariotti, G., 2016. Revisiting salt marsh resilience to sea level rise: are ponds responsible for permanent land loss? J. Geophys. Res. Earth Surf 1391–1407. https://doi.org/10.1002/2016JF003900.
- Mariotti, G., Huang, H., Xue, Z., Li, B., Justic, D., Zang, Z., 2018. Biased Wind Measurements in Estuarine Waters. J. Geophys. Res. Ocean. 1–11. https://doi.org/ 10.1029/2017JC013748.
- McClenachan, G., Eugene Turner, R., Tweel, A.W., 2013. Effects of oil on the rate and trajectory of Louisiana marsh shoreline erosion. Environ. Res. Lett. 8. https://doi.org/10.1088/1748-9326/8/4/044030.
- McLoughlin, S.M., Wiberg, P.L., Safak, I., McGlathery, K.J., 2015. Rates and Forcing of Marsh Edge Erosion in a Shallow Coastal Bay. Estuar. Coasts 38, 620–638. https://doi.org/10.1007/s12237-014-9841-2.
- Morton, R.A., Bernier, J.C., Kelso, K.W., 2009. Recent Subsidence and Erosion at Diverse Wetland Sites in the Southeasern Mississippi Delta Plain. US Geological Series Open File Report.
- Nyman, J.A., Carloss, M., Delaune, R.D., Patrick, H., 1994. Erosion rather than plant dieback as the mechanism of marsh loss in a n estuarine marsh. Earth Surf. Process. Landforms 19, 69–84.
- Ortiz, A.C., Roy, S., Edmonds, D.A., 2017. Land loss by pond expansion on the Mississippi River Delta Plain. Geophys. Res. Lett. 44, 3635–3642. https://doi.org/10.1002/2017c1.073079
- Pendleton, L., Donato, D.C., Murray, B.C., Crooks, S., Jenkins, W.A., Sifleet, S., Craft, C., Fourqurean, J.W., Kauffman, J.B., Marbà, N., Megonigal, P., Pidgeon, E., Herr, D., Gordon, D., Baldera, A., 2012. Estimating Global "Blue Carbon" Emissions from Conversion and Degradation of Vegetated Coastal Ecosystems. PLoS One 7. https://doi.org/10.1371/journal.pone.0043542.
- Penland, S., Ramsey, K.E., 1990. Relative sea-level rise in Louisiana and the Gulf of Mexico: 1908-1988. J. Coast. Reserch 6, 323–342.
- Peyronnin, N.S., Caffey, R.H., Cowan, J.H., Justic, D., Kolker, A.S., Laska, S.B., McCorquodale, A., Melancon, E., Nyman, J.A., Twilley, R.R., Visser, J.M., White, J.R., Wilkins, J.G., 2017. Optimizing sediment diversion operations: Working group recommendations for integrating complex ecological and social landscape interactions. Water (Switzerland) 9. https://doi.org/10.3390/w9060368.
- Priestas, A.M., Mariotti, G., Leonardi, N., Fagherazzi, S., 2015. Coupled Wave Energy and

- Erosion Dynamics along a Salt Marsh Boundary, Hog Island Bay, Virginia, USA. J. Mar. Sci. Eng. 3, 1041–1065. https://doi.org/10.3390/jmse3031041.
- Reddy, K., DeLaune, R., 2008. Biogeochemistry of Wetlands. CRC Press, Boca Raton.
 Reimer, P.J., Bard, E., Bayliss, A., Beck, J.W., Blackwell, P.G., Bronk, C., Caitlin, R., Hai,
 E.B., Edwards, R.L., et al., 2013. Intcal13 and marine13 radiocarbon age calibration curves 0 50,000 years cal bp. Radiocarbon 55, 1869–1887.
- Roberts, H.H., DeLaune, R.D., White, J.R., Li, C., Sasser, C.E., Braud, D., Weeks, E., Khalid, S., 2015. Floods and Cold Front Passages:Impacts on Coastal Marshes in a River Diversion Setting (Wax Lake Delta, Louisiana). J. Coast. Res. 31 (5), 1057–1068
- Rogers, K., Kelleway, J.J., Saintilan, N., Megonigal, J.P., Adams, J.B., Holmquist, J.R., Lu, M., Schile-Beers, L., Zawadzki, A., Mazumder, D., Woodroffe, C.D., 2019. Wetland carbon storage controlled by millennial-scale variation in relative sea-level rise. Nature 567, 91–95. https://doi.org/10.1038/s41586-019-0951-7.
- Schuerch, M., Spencer, T., Temmerman, S., Kirwan, M.L., Wolff, C., Lincke, D., McOwen, C.J., Pickering, M.D., Reef, R., Vafeidis, A.T., Hinkel, J., Nicholls, R.J., Brown, S., 2018. Future response of global coastal wetlands to sea-level rise. Nature 561, 231–234. https://doi.org/10.1038/s41586-018-0476-5.
- Sharma, S., Goff, J., Moody, R.M., McDonald, A., Byron, D., Heck, K.L., Powers, S.P., Ferraro, C., Cebrian, J., 2016. Effects of shoreline dynamics on saltmarsh vegetation. PLoS One 11. https://doi.org/10.1371/journal.pone.0159814.
- Sorensen, R.M., 2006. Basic Coastal Engineering, third ed. Springer SciencebBusiness Media, Inc., NY, USA.
- Spivak, A.C., Gosselin, K., Howard, E., Mariotti, G., Forbrich, I., Stanley, R., Sylva, S.P., 2017. Shallow ponds are heterogeneous habitats within a temperate salt marsh ecosystem. J. Geophys. Res. Biogeosciences 122, 1371–1384. https://doi.org/10. 1002/2017.IG003780
- Steinmuller, H.E., Chambers, L.G., 2019. Characterization of coastal wetland soil organic matter: Implications for wetland submergence. Sci. Total Environ. 677, 648–659. https://doi.org/10.1016/j.scitotenv.2019.04.405.
- Steinmuller, H.E., Dittmer, K.M., White, J.R., Chambers, L.G., 2019. Understanding the fate of soil organic matter in submerging coastal wetland soils: A microcosm approach. Geoderma. https://doi.org/10.1016/j.geoderma.2018.08.020.
- Su, X., Nilsson, C., Pilotto, F., Liu, S., Shi, S., Zeng, B., 2017. Soil erosion and deposition in the new shorelines of the Three Gorges Reservoir. Sci. Total Environ. 599–600, 1485–1492. https://doi.org/10.1016/j.scitotenv.2017.05.001.
- Theuerkauf, E.J., Stephens, J.D., Ridge, J.T., Fodrie, F.J., Rodriguez, A.B., 2015. Carbon export from fringing saltmarsh shoreline erosion overwhelms carbon storage across a critical width threshold. Estuar. Coast Shelf Sci. 164, 367–378. https://doi.org/10.1016/i.ecss.2015.08.001.
- Tonelli, M., Fagherazzi, S., Petti, M., 2010. Modeling wave impact on salt marsh boundaries. J. Geophys. Res. Ocean. 115, 1–17. https://doi.org/10.1029/20091C006026
- Turner, R.E., McClenachan, G., Tweel, A.W., 2016. Islands in the oil: Quantifying salt marsh shoreline erosion after the Deepwater Horizon oiling. Mar. Pollut. Bull. 110, 316–323. https://doi.org/10.1016/j.marpolbul.2016.06.046.
- USEPA, 1993. Methods for Determination of Inorganic Substances in Environmental Samples. PA/600/R-93/100. (Washington D.C).
- Vaccare, J., Meselhe, E., White, J.R., 2019. The denitrification potential of eroding wetlands in Barataria Bay, LA, USA: Implications for river reconnection. Sci. Total Environ. 66, 529–537. https://doi.org/10.1016/j.scitotenv.2019.05.475.
- Valentine, K., Mariotti, G., 2019. Wind-driven water level fluctuations drive marsh edge erosion variability in microtidal coastal bays. Cont. Shelf Res. 176, 76–89. https:// doi.org/10.1016/j.csr.2019.03.002.
- Wang, H., van der Wal, D., Li, X., van Belzen, J., Herman, P.M.J., Hu, Z., Ge, Z., Zhang, L., Bouma, T.J., 2017. Zooming in and out: Scale dependence of extrinsic and intrinsic factors affecting salt marsh erosion. J. Geophys. Res. Earth Surf. 122, 1455–1470. https://doi.org/10.1002/2016JF004193.
- White, J.R., Reddy, K.R., 1999. Influence of nitrate and phosphorus loading on denitrifying enzyme activity in Everglades wetland soils. Soil Sci. Soc. Am. J. 63, 1945–1954. https://doi.org/10.2136/sssaj1999.6361945x.
- White, J.R., Reddy, K.R., 2001. Influence of selected inorganic electron acceptors on organic nitrogen mineralization in everglades soils. Soil Sci. Soc. Am. J. 65, 941–948.
- Wilson, C.A., Allison, M.A., 2008. An equilibrium profile model for retreating marsh shorelines in southeast Louisiana. Estuar. Coast Shelf Sci. 80, 483–494. https://doi. org/10.1016/j.ecss.2008.09.004.
- Wolters, M., Bakker, J.P., Bertness, M.D., Jefferies, R.L., Möller, I., 2005. Saltmarsh erosion and restoration in south-east England: Squeezing the evidence requires realignment. J. Appl. Ecol. 42, 844–851. https://doi.org/10.1111/j.1365-2664.2005. 01080.x.
- Wood, S.E., White, J.R., Armbruster, C.K., 2017. Microbial processes linked to soil organic matter in a restored and natural coastal wetland in Barataria Bay. Louisiana. Ecol. Eng. 106, 507–514. https://doi.org/10.1016/j.ecoleng.2017.06.028.